



Temperature Effect on Photovoltaic Modules Power Drop

Qais Mohammed Aish

Institute of Technology/ Baghdad

Email: Abdgold171@yahoo.com

(Received 20 February 2014; accepted 25 January 2015)

Abstract

In order to determine what type of photovoltaic solar module could best be used in a thermoelectric photovoltaic power generation. Changing in powers due to higher temperatures (25°C, 35°C, and 45°C) have been done for three types of solar modules: monocrystalline, polycrystalline, and copper indium gallium (di) selenide (CIGS). The Prova 200 solar panel analyzer is used for the professional testing of three solar modules at different ambient temperatures; 25°C, 35°C, and 45°C and solar radiation range 100-1000 W/m². Copper indium gallium (di) selenide module has the lowest power drop (with the average percentage power drop 0.38%/°C) while monocrystalline module has the highest power drop (with the average percentage power drop 0.54%/°C), while polycrystalline module has a percentage power drop of 0.49%/°C.

Keywords: Energy gap, PV modules, PV power, Temperature dependence.

1. Introduction

Photovoltaics, or solar panels that produce electricity, are affected by their operating temperature, which is primarily a product of the ambient air temperature as well as the level of sunlight. The pronounced effect that the operating temperature of a photovoltaic (PV) cell/module has upon its electrical efficiency is well documented. There are many correlations expressing T_c , the PV cell temperature, as a function of weather variables such as the ambient temperature, T_a , and the local wind speed, V_w , as well as the solar radiation flux/irradiance, G_T , with material and system-dependent properties as parameters, e.g., glazing-cover transmittance, τ , plate absorptance, α etc [1].

An equally large number of correlations expressing the temperature dependence of the PV module's electrical efficiency, η_c , can also be retrieved, although many of them assume the familiar linear form, differing only in the numerical values of the relevant parameters

which, as expected, are material and system dependent. Many correlations in this category express instead the module's maximum electrical power, P_m , which is simply related to τ_c through the latter's definition ($\eta_c = P_m$ (under standard test conditions; 25 °C and $G_T=1000$ w/m²) / AG_T), with A being the aperture area), and form the basis of various performance rating procedures.

2. PV Power Output Dependence on Module Operating Temperature

The prediction of PV module performance in terms of electrical power output in the field, that is, the deviation from the standard test conditions reported by the manufacturer of the module. For example, a recently proposed correlation for PV power is in which τ_{pv} is the transmittance of the PV cells outside layers [2a,b]. A number of correlations found in the literature for PV electrical power as a function of cell/module operating temperature and basic environmental variables. Many of them are linear, while others

are more complex, such as the following nonlinear multivariable regression equation [3] ,

$$P_{mp} = d_1 + d_2 T_c + d_3 [\ln(G_T)]^m d_4 T_c [\ln(G_T)]^m \quad \dots(1)$$

resulting from an analysis which addresses the fact that the cells within a module are not identical. (Here, d_j , $j = 1-4$ and m are model parameters.) Another unusual nonlinear correlation [4] gives a correction coefficient for the output power of a water cooled PV system, namely.

$$P = V_c T_c \left[1 - \frac{G_T - 500}{2 \cdot 10^{-4}} + \frac{C_{T_c}}{4 \cdot 10^4} (50 - T_c)^2 \right] \quad \dots(2)$$

In which V_c and I_c are the output voltage and current, respectively, while the parameter C_{T_c} takes values 1 or 3, for values of T_c below or above 50°C , respectively. With regard to the wind's indirectly beneficial effect of lowering the operating temperature by forced convection and, thus, increasing the power output of the modules, the available model [5], is of the form:

$$P = G_T (b_1 + b_2 G_2 + b_3 T_a + b_4 V_f) \quad \dots(3)$$

In this nonlinear equation, V_f is the free-stream local wind speed, i.e., it is measured at a height of 10 m above ground, and the regression coefficients b_j , $j = 1-4$ are determined using solar radiation flux values above 500 W/m^2 [6].

The steady-state power balance determines cell temperature: the input is the absorbed luminous power, which is partially converted into useful electrical output and the rest is dissipated into the surroundings. Convection is the main mechanism for heat dissipation in terrestrial, flat plate applications, and radiation is the second non-negligible mechanism of heat dissipation. A common simplifying assumption is made that the cell-ambient temperature drop increases linearly with irradiance. The coefficient depends on module installation, wind speed, ambient humidity and so on, though a single value is used to characterize a module type [7]. This information is contained in the Nominal Operating Cell Temperature (NOCT), which is defined as the cell temperature is measured under open-circuit when the ambient temperature is 20°C , irradiance is 0.8 kW/m^2 and wind speed is 1 m/s . T_{NOCT} usually values around 45°C . For variations in ambient temperature and irradiance the cell temperature (in $^\circ\text{C}$) can be estimated quite accurately with the linear approximation [8];

$$T_c = T_a + \frac{T_{NOCT} - 20}{0.8 \text{ kW/m}^2} G_T \quad \dots(4)$$

Solar panels work best in certain weather conditions, but since the weather is always changing and as engineers are installing solar panels all over the world in different climate regions, most panels do not operating under ideal conditions. That is why it is important for engineers to understand how panels react to different weather conditions. With this knowledge, they can design ways to improve the efficiency of solar panels that operate in non-optimal conditions.

In some cases, they design cooling systems to keep the panels within certain temperatures. For example, solar power plants in extremely hot climates may pass a cool liquid behind the panels to pull away heat and keep the panels cool. This is similar to how your body might sweat as a way to stay cool if you were on that run in the 110°F air temperature [8].

While it is important to know the temperature of a solar PV panel to predict its power output, it is also important to know the PV panel material because the efficiencies of different materials have varied levels of dependence on temperature. Therefore, a PV system must be engineered not only according to the maximum, minimum and average environmental temperatures at each location, but also with an understanding of the materials used in the PV panel. The temperature dependence of a material is described with a temperature coefficient. For polycrystalline PV panels, if the temperature decreases by one degree Celsius, the voltage increases by 0.12 V so the temperature coefficient is 0.12 V/C . Effect of temperature on module output relative to standard condition ($T_c=25^\circ\text{C}$ and $G_T= 1000 \text{ W/m}^2$) is available in Fig.1

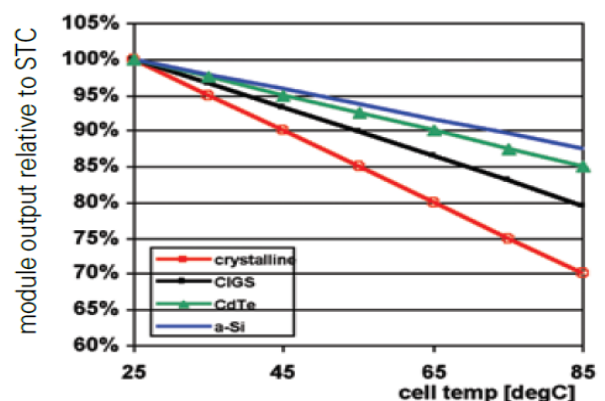


Fig. 1. The effects of a negative temperature coefficient of power on PV module performance [9].

3. Experimental Measurements

Three types of photovoltaic solar cells are selected to study temperature effect on the output power drop of the solar modules:

1. Monocrystalline cells are cut from a single crystal of silicon- they are effectively a slice from a crystal. In appearance, it will have a smooth texture and you will be able to see the thickness of the slice. These are the most efficient and the most expensive to produce [10]. They are also rigid and must be mounted in a rigid frame to protect them (see Fig.2).



Fig. 2. Monocrystalline panel.

2. Polycrystalline (or Multicrystalline) cells are effectively a slice cut from a block of silicon, consisting of a large number of crystals. They have a speckled reflective appearance and again you can see the thickness of the slice [10]. These cells are slightly less efficient and slightly less expensive than monocrystalline cells and again need to be mounted in a rigid frame (see Fig. 3).



Fig. 3. Polycrystalline panel.

3. Copper indium gallium (di) selenide (CIGS) is a I-III-VI₂ semiconductor material composed of copper, indium, gallium, and

selenium. The material is a solid solution of copper indium selenide (often abbreviated "CIS") and copper gallium selenide[10]. It has a chemical formula of $CuIn_xGa_{(1-x)}Se_2$ where the value of x can vary from 1 (pure copper indium selenide) to 0 (pure copper gallium selenide). CIGS is a tetrahedrally bonded semiconductor, with the chalcopyrite crystal structure, and a band gap varying continuously with x from about 1.0 eV (for copper indium selenide) to about 1.7 eV (for copper gallium selenide)(see Fig.4).

Among many uses, CIGS is best known as an alternate solar cell material in thin-film solar cells[10]. In this role, CIGS has the advantages of being able to be deposited on flexible substrate materials, producing highly flexible, lightweight solar panels. Improvements in efficiency have made CIGS a leader among alternative cell materials.



Fig. 4. Copper indium gallium (di) selenide (CIGS).

3.1. Experimental Procedure

The Prova 200 solar panel analyzer (Fig.5) is used for the professional testing and maintenance of solar panels and modules. In addition to maintenance and installation of solar panels, the Prova 200 solar panel analyzer can be used in the manufacturing and research of solar panels and cells. Table 1 provides the general specification of Prova 200. The portability of this device means that it is also useful in quality assurance at various stages on the production line and can be taken from one location to another. When used in the installation of solar panels, the Prova 200 solar panel analyzer assists in determining the proper inverter size as well as optimum power output position of panels and helps identify defective cells or panels that have worn out over time. The solar panel analyzer also provides the user with current and voltage (I-V) test curves, maximum solar power as well as current and voltage. Solar cell efficiencies are also easily determined using the unit. Prova 200 have a software supply by

manufacturing company to calibrate the device automatically. This process is done periodically the device is connect with the internet.



Fig. 5. The Prova 200 solar panel analyzer.

Table 1, General Specifications of Prova 200.

Battery type	Rechargeable, 2500mAh(1.2V)*8
AC Adaptor	AC 110V or 220V input DC 12V / 1~3A output
Dimension	257(L) * 155(W) *57(H) mm
Weight	1160g / 40 Ooz
Operation environment	0°C ~ 50°C,85% RH
Temperature coefficient	0.1% of full scale/ C (<18C or >28C)
Storage environment	-20C ~ 60C ,75%C
accessories	User manual * 1, AC adaptor*1 Optical USB cable*1 Software CD *1, software manual *1 Kelvin clips(6A max) *1 set

Table 2, Solar modules specifications.

Module type	Area, m ²	V _{oc} , v	I _{sc} , A	Peak power , w	Peak voltage , v	Peak current , A	Energy gap, eV	Production date
CIGS	0.03	11	0.33	1.8	6.6	0.28	1.35	2013
Monocrystalline	0.36	19.5	2.8	35	15.8	2.3	1.12	2013
Polycrystalline	1	22	8.1	130	18.5	6.0	1.75	2013

3.1.2. Solar panel Parameters Measure

The main parameters that characterize a photovoltaic panel (Fig.4) are:

1. Short circuit current (I_{sc}): the maximum current provided by the panel when the connectors are short circuited.
2. Open circuit voltage (V_{oc}): the maximum voltage that the panel provides when the terminals are not connected to any load (an open circuit).

3.1.1. Connecting Wires (Connectors)

The terminals of the solar cell are connected as in Fig.6. In this work, the system of measurements is consists of silicon solar cell as it is presented in Fig.4. Fig.4 shows the set-up of our experiment. It is based on the simple solar-cell experiment. Table 2 gives the general specification of this cell.

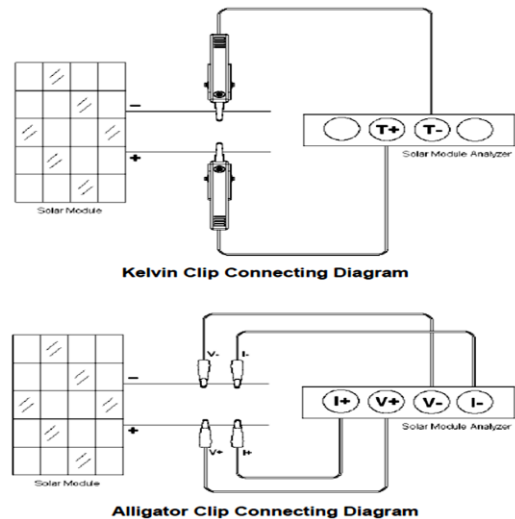


Fig. 6. Wires connections.

3. Maximum power point (P_{max}): the point where the power supplied by the panel is at maximum, where P_{max} = I_{max} x V_{max}. The maximum power point of a panel is measured in Watts (W) or peak Watts (W_p). It is important not to forget that in normal conditions the panel will not work at peak conditions, as the voltage of operation is fixed by the load or the regulator. Typical values of V_{max} and I_{max} should be a bit smaller than the I_{sc} and V_{oc}.

4. Fill factor (FF): the relation between the maximum power that the panel can actually provide and the product $I_{SC} \cdot V_{OC}$. This gives you an idea of the quality of the panel because it is an indication of the type of IV characteristic curve. The closer FF is to 1,

the more power a panel can provide. Common values usually are between 0.7 and 0.8.

5. Efficiency (η): the ratio between the maximum electrical power that the panel can give to the load and the power of the solar radiation (P_L) incident on the panel. This is normally around 10-12%, depending on the type of cells (monocrystalline, polycrystalline, amorphous or thin film). Considering the definitions of point of maximum power and the fill factor we see that:

$$\eta = P_{max}/P_L = FF \cdot I_{sc} \cdot V_{oc} / P_L \quad \dots (6)$$

The prova 200 experimental measurement steps are as follow:

- 1- Connect the solar panel solar panel as in Fig.6
- 2- Connect the solar panel terminal T_1 and T_2 with the prova 200 device (Kelvin clip connection) as in Fig. 6
- 3- Input the value of surface area in square meters of the panel and the measured values of solar radiation intensity in W/m^2
- 4- The measurements is made at a sunny day and at different time intervals of the day so as to get the adjusted values of solar radiation intensity (100, 200, 300, 400, 500, 600, 700, 800, 900, and 1000 W/m^2 and solar cell temperatures (25°C, 35°C, and 45°C).
- 5- Prova 200 will be made auto scanning at a variable load in ohm (0 to ∞)
- 6- Prova 200 output are: Voltage (V_{now}), Open circuit voltage (V_{OC}), Short circuit current (I_{SC}), , Maximum power point (P_{max}), Maximum current (I_{max}), Maximumvoltage (V^{max}), Fill factor (FF), and Efficiency (η).

4. Results and Discussion

The measuring results of the commercial available solar cells from different manufacturers are presented. Cell samples have been investigated regarding their I-V characteristics at different solar intensities in a range 100-1000 W/m^2 and the ambient temperature between (25°C, 35°C, and 45°C). All the measurements and the characteristics of these cells have been made within the date of September and November 2013. The data obtained for I-V characteristics and P-V curve for three types of solar modules;

monocrystalline, polycrystalline and copper indium gallium (di)selenide under the specific solar radiation intensities (100-1000 W/m^2) and ambient temperatures, 25°C,35°C, and 45°C are shown in Tables 3 to 5.

Solar cells powers vary under temperature changes. The change in temperature (increasing values) will affect the power output from the cells (Because of the problem of loss of electricity as a result of heat buildup and non-ideal behavior of semiconductor with the corresponding temperature increase). The voltage is highly dependent on the temperature and an increase in temperature will decrease the voltage. Equation 1, Equation 2 and Equation 3 repent the relationship between solar module power and other environment parameters (solar radiation G, ambient temperature T_a , solar module temperature T_c ; which is strongly function with ambient temperature T_a (see Equation 4), and wind speed v_f). Fig.7a, Fig.8a, and Fig.9a show the effect of temperature on I-V characteristic of three PV modules at constant solar radiation(1000 W/m^2) and different ambient temperatures; 25°C,35°C, and 45°C . With decreasing temperatures, PV currents decrease slightly but PV voltage increase clearly to the all corresponding PV module. As Fig.7b, Fig.8b, and Fig.9b indicate, output powers of photovoltaic modules increase with decreasing the selected temperatures (i.e. 25°C, 35°C, and 45°C). However, Copper indium gallium (di)selenide has the lowest power drop (with the average percentage power drop 0.38%/°C) while monocrystalline has the highest power drop (with the average percentage power drop 0.54%/°C) according to the tabulated power values in Tables 3,4, and 5). The percentage of power drop of polycrystalline module is 0.49%/°C). Radziemska [11] found for the monocrystalline module that the average output power drop is equal to 0.66%/°C. It has been found that the maximum power density of the two modules decreases with increasing module temperature, where the maximum power density of the mono-crystalline and the poly-crystalline modules for temperature=10°C was 43.4 mW/cm^2 and 48.76 mW/cm^2 , respectively. Increasing the temperature to 50°C causes the decrease of the power by 25% and 14% to reach values 36.32 mW/cm^2 and 41.88 mW/cm^2 respectively [12]. This results of ref[11] agrees with proposed results that monocrystalline module has the largest values of power drop as compared with polycrystallane module.

One should expect any device utilizing semiconductors to be quite sensitive to

temperature deviations from normal operating temperatures, and solar cells are no exception. An increase in the operating temperature of a solar cell (or the corresponding ambient temperature) typically has the effect of slightly increasing the cell's short-circuit current and significantly

decreasing the cell voltage. Therefore, as the temperature of the solar cell rises, the result is that the maximum efficiency decreases (the area of the power rectangle under the VI curve decreases).

Table 3,
CIGS electrical measured data at different solar intensities (100-1000 W/m²) and different temperatures, 25 °C, 35 °C, and 45 °C.

G w/m ²	T °C	V _{now} v	V _{oc} v	I _{SC} A	P _{max} w	V _{max} v	I _{max} A	% η	FF
100	25	9.42	9.22	0.030	0.19	7.12	0.026	8.63	0.67
	35	9.332	8.76	0.032	0.188	6.76	0.027	7.85	0.654
	45	9.866	8.545	0.0347	0.183	6.425	0.028	6.125	0.619
200	25	9.44	9.41	0.046	0.298	7.48	0.040	8.51	0.66
	35	9.21	9.01	0.045	0.278	7.233	0.038	5.689	0.645
	45	9.048	9.058	0.0439	0.250	6.921	0.0362	4.175	0.630
300	25	9.84	9.81	0.090	0.583	7.41	0.078	8.43	0.65
	35	9.571	9.561	0.076	0.443	7.19	0.061	6.34	0.64
	45	9.315	9.309	0.0682	0.412	6.985	0.059	4.586	0.650
400	25	9.92	9.91	0.105	0.678	7.31	0.092	7.73	0.64
	35	9.435	9.567	0.095	0.521	7.201	0.072	5.471	0.639
	45	9.362	9.359	0.0791	0.484	7.182	0.067	4.033	0.633
500	25	10.04	10.01	0.133	0.843	7.17	0.117	7.30	0.63
	35	9.89	9.893	0.122	0.758	7.166	0.105	6.54	0.649
	45	9.372	9.606	0.119	0.745	7.158	0.104	4.967	0.650
600	25	10.11	10.09	0.157	0.970	6.93	0.140	7.30	0.61
	35	9.78	9.78	0.143	0.837	7.102	0.117	6.235	0.6211
	45	9.587	9.618	0.134	0.825	7.328	0.112	4.584	0.639
700	25	10.14	10.12	0.173	1.093	6.92	0.150	6.4	0.59
	35	9.43	9.78	0.166	0.989	6.988	0.141	5.89	0.604
	45	8.730	9.656	0.160	0.966	7.047	0.137	4.600	0.622
800	25	10.20	10.18	0.196	1.146	6.73	0.170	6.23	0.57
	35	9.71	9.98	0.178	1.042	6.76	0.154	5.67	0.611
	45	9.596	9.619	0.165	0.980	6.780	0.144	4.084	0.615
900	25	10.23	10.22	0.217	1.229	6.58	0.186	6.14	0.55
	35	10.01	9.897	0.201	1.186	6.863	0.172	5.43	0.596
	45	9.972	9.674	0.190	1.139	6.902	0.165	4.220	0.618
1000	25	10.37	10.36	0.256	1.394	6.42	0.217	6.06	0.52
	35	9.36	10.01	0.237	1.310	6.642	0.197	5.246	0.567
	45	8.428	9.995	0.215	1.254	6.883	0.182	4.188	0.582

Table 4,
Monocrystalline electrical measured data at different solar intensities (100-1000 W/m²) and different temperatures, 25 °C, 35 °C, and 45 °C.

G w/m²	T °C	V_{now} v	V_{oc} v	I_{sc} A	P_{max} w	V_{max} v	I_{max} A	η %	FF
100	25	16.2	16.19	0.196	1.5	11.7	0.131	4.21	0.48
	35	15.98	15.69	0.256	2.34	11.88	0.196	6.74	0.521
	45	15.43	15.55	0.339	2.966	11.94	0.25	8.322	0.568
200	25	17.42	17.4	0.383	4.04	13.58	0.299	5.54	0.61
	35	16.58	16.68	0.413	4.16	12.92	0.32	5.893	0.621
	45	15.79	15.70	4670.	4.603	12.31	0.373	6.393	0.637
300	25	17.99	17.94	0.556	6.52	14.4	0.426	5.90	0.65
	35	16.59	16.567	0.52	6.21	13.55	0.458	4.78	0.645
	45	16.05	15.97	0.5	5.082	12.59	0.403	4.7.5	0.636
400	25	18.2	18.18	0.825	10.1	14.63	0.693	6.53	0.67
	35	17.94	17.409	0.805	9.77	14.01	0.697	6.34	0.6632
	45	16.64	16.61	0.764	8.256	13.18	0.626	5.733	0.65.
500	25	18.3	18.25	0.972	12.6	14.71	0.73	6.42	0.79
	35	17.345	17.54	0.989	11.23	13.69	0.820	6.432	0.734
	45	16.72	16.69	1.028	11.61	13.34	0.870	6.454	0.676
600	25	18.4	18.36	1.106	14.1	14.81	0.952	6.37	0.69
	35	17.89	17.643	1.118	13.10	14.21	0.921	6.034	0.689
	45	16.85	16.83	1.127	12.91	13.52	0.954	5.977	0.680
700	25	18.5	18.49	1.23	15.97	15.03	1.06	6.23	0.69
	35	17.98	17.567	1.278	15.63	14.98	1.04	6.196	0.684
	45	17.04	17.02	1.342	15.59	13.59	1.154	6.188	0.682
800	25	18.8	18.79	1.62	21.5	15.3	1.4	7.3	0.7
	35	17.694	18.045	1.56	19.74	14.76	1.33	6.45	0.697
	45	17.09	17.08	1.439	16.85	13.61	1.238	5.853	0.685
900	25	18.89	18.88	1.71	22.9	15.2	1.507	6.9	0.7
	35	17.67	17.578	1.687	20.33	14.56	1.39	6.56	0.69
	45	17.11	17.13	1.658	19.50	13.67	1.426	6.020	0.686
1000	25	19.05	19.05	1.95	26.4	15.4	1.72	7.2	0.71
	35	18.56	18.49	1.934	23.78	14.63	1.625	6.84	0.689
	45	17.15	17.16	1.928	22.67	13.51	1.684	6.323	0.687

Table 5,
Polycrystalline electrical measured data at different solar intensities (100-1000 W/m²) and different temperatures, 25 °C, 35 °C, and 45 °C.

G w/m ²	T °C	V _{now} V	V _{oc} V	I _{sc} A	P _{max} W	V _{max} V	I _{max} A	η %	FF
100	25	17.6	17.5	1.2	13.92	17.40	0.8	13.92	0.66
	35	18.54	17.89	1.15	13.88	16.32	0.85	14.054	0.723
	45	19.31	18.69	1.050	14.88	15.89	0.931	14.90	0.758
200	25	19.10	19.00	1.800	28.00	17.50	1.600	14.00	0.81
	35	19.04	18.998	1.76	23.54	16.88	1.39	10.48	0.788
	45	18.91	18.91	1.720	18.42	16.23	1.135	9.221	0.766
300	25	20.50	20.50	2.5	42.05	17.52	2.4	10.5	0.82
	35	19.78	20.056	2.32	33.761	16.922	1.995	9.78	0.794
	45	19.23	19.23	1.905	28.41	16.21	1.752	9.480	0.755
400	25	21.01	21.00	3.1	51.3	17.7	2.9	12.8	0.78
	35	20.45	20.67	3.067	40.81	17.21	2.371	11.34	0.778
	45	19.40	19.42	2.513	37.38	16.28	2.295	9.356	0.765
500	25	21.09	21.08	3.52	54.9	17.72	3.1	10.98	0.73
	35	20.23	20.862	3	49.60	17.32	2.86	9.65	0.737
	45	19.46	19.46	2.965	43.11	16.77	2.569	8.631	0.747
600	25	21.14	21.13	3.56	63.9	17.76	3.5	10.6	0.84
	35	20.78	20.46	3.87	61.22	17.22	3.55	10.34	0.789
	45	19.65	19.67	4.043	60.36	16.22	3.720	10.07	0.758
700	25	21.25	21.24	4.5	76.9	17.8	4.3	10.9	0.8
	35	20.68	20.46	4.456	73.89	16.92	4.367	9.67	0.778
	45	19.61	19.63	4.332	64.35	16.26	3.956	9.202	0.756
800	25	21.4	21.39	5.06	83.84	17.84	4.7	10.48	0.77
	35	20.976	20.56	5.21	81.76	17.35	4.712	10.04	0.765
	45	19.62	19.56	5.332	78.82	16.06	4.906	9.863	0.752
900	25	21.51	21.52	5.6	94.42	18.02	5.24	10.49	0.78
	35	20.47	20.567	5.678	91.442	17.47	5.234	9.678	0.762
	45	19.59	19.59	5.719	84.40	16.04	5.262	9.378	0.753
1000	25	21.6	21.59	5.8	100.7	18.31	5.5	10.07	0.8
	35	20.68	20.78	5.98	97.87	17.45	5.6	9.67	0.793
	45	19.49	19.65	6.276	92.10	15.95	5.744	9.220	0.746

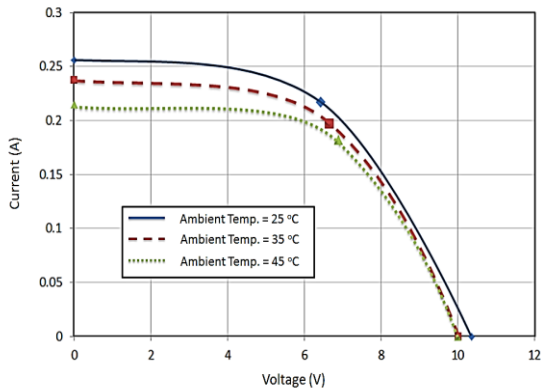


Fig. 7a. Output I-V characteristics of the Copper indium gallium (di) selenide with different temperatures and constant solar radiation (1000 W/m²).

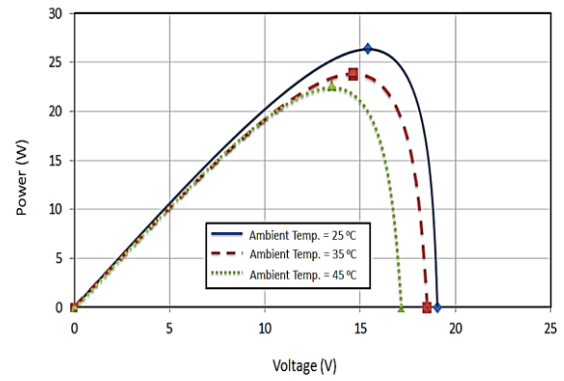


Fig. 8b. Output P-V characteristics of Monocrystalline with different temperatures and constant solar radiation (1000 W/m²).

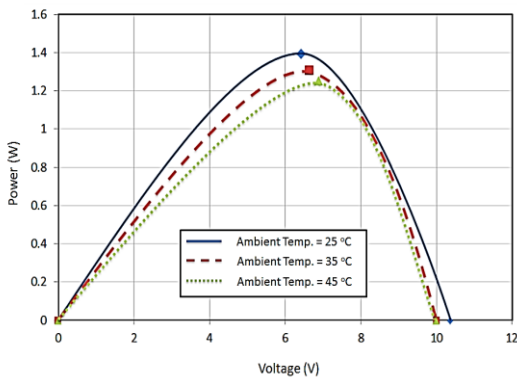


Fig. 7b. Output P-V characteristics of the Copper indium gallium (di) selenide with different temperatures and constant solar radiation (1000 W/m²).

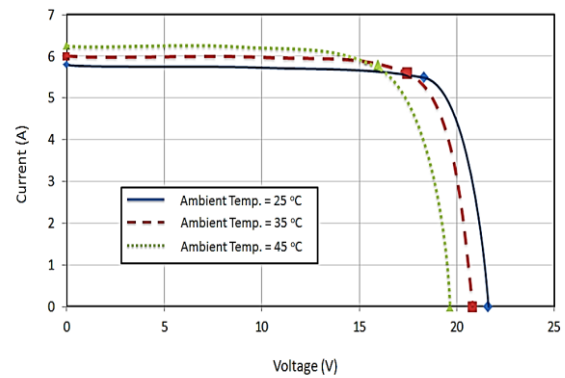


Fig. 9a. Output I-V characteristics of polycrystalline with different temperatures and constant solar radiation (1000 W/m²).

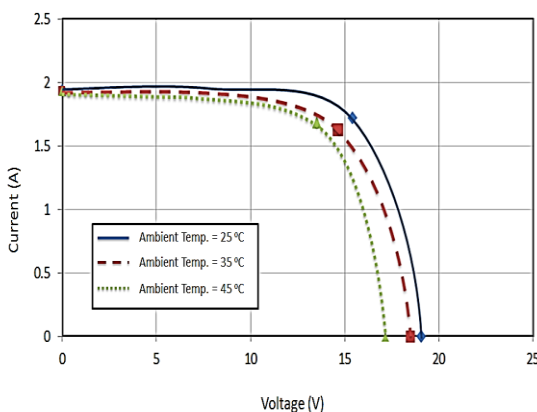


Fig. 8a. Output I-V characteristics of Monocrystalline with different temperatures and constant solar radiation (1000 W/m²).

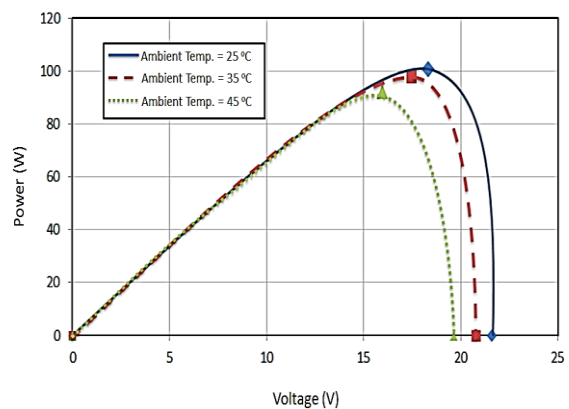


Fig. 9b. Output P-V characteristics of polycrystalline with different temperatures and constant solar radiation (1000 W/m²).

5. Conclusions

The operating temperature plays a central role in the photovoltaic conversion process. The power outputs of PV modules depend on the operating temperature, decreasing with increasing the ambient temperatures. According to the experimental measurements solar modules powers decrease against temperatures increasing. It became clear that as the temperature raises the power drops. Compare to the experimental measurements, in regard to power drop percentage per temperature vary from module to another, which are for Monocrystalline module > Polycrystalline module > pCopper indium gallium (di)selenide.

Notation

A	ideality factor
A	aperture surface area of PV module (m ²)
G _T	solar radiation flux (irradiance) on module plane (W/m ²)
P	electrical power (W)
FF	Fill factor
G	Solar radiation, w/m ²
I _L	Photocurrent, A
I _{maxp} I _{mp}	Maximum Current at P _{max} , mA
I _o	Saturation current, A
I _p	Operating current, A
I _{sc}	Current at short circuit, mA
P _L	Power of Solar radiation, w
P _{max}	Maximum Solar Power, w
R _L	Load resistance, Ω
T _a	Ambient temperature, °C
T _c	Cell/module operating temperature, °C
T _{NOCT}	Nominal operating cell temperature, °C
V _{maxp}	Maximum Voltage at P _{max} , V
V _{mp}	
V	Voltage (V)
V _f	Free stream wind speed (m/s)
V _w	Wind speed at monitored surface (m/s)
V _{oc}	Voltage at open circuit, V

Greek letters

η	cell/module electrical efficiency, %
τ	solar transmittance of glazing

Subscripts

0	at SRC
a	ambient
b	back side
c	cell (module)

f	free stream
L	loss
m	maximum, at maximum power point
oc	open circuit
ref	reference value, at reference conditions
sc	short circuit

6. Reference

- [1] Skoplaki E. and J.A. Palyvos, "On the temperature dependence of photovoltaic module electrical performance: A review of efficiency/power correlations", *Solar Energy* 83, 614–624, 2009.
- [2-a] Jie, J., Hua, Y., Gang, P., Bin, J., Wei, H.. Study of PV-Trombe wall assisted with DC fan. *Building and Environment* 42, 3529–3539, 2007a.
- [2-b] Jie, J., Hua, Y., Wei, H., Gang, P., Jianping, L., Bin, J.. Modeling of a novel Trombe wall with PV cells. *Building and Environment* 42, 1544–1552, 2007b.
- [3] Rosell, J.I., Ibañez, M.. Modelling power output in photovoltaic modules for outdoor operating conditions. *Energy Conversion and Management* 47, 2424–2430, 2006.
- [4] Furushima, K., Nawata, Y., Sadatomi, M., Prediction of photovoltaic power output considering weather effects. In: *ASES Conference SOLAR 2006 – Renewable Energy Key to Climate Recovery*. July 7–13, Denver, Colorado, 2006.
- [5] Farmer, B.K., PVUSA Model Technical Specification for a Turnkey Photovoltaic Power System. Appendix C, p. c2, 1992
- [6] Meyer, E.L., van Dyk, E.E.. Development of energy model based on total daily irradiation and maximum ambient temperature. *Renewable Energy* 21, 37–47, 2000.
- [7] Fesharaki V., Jafari, Majid Dehghani, J. Jafari Fesharaki The Effect of Temperature on Photovoltaic Cell Efficiency, *Proceedings of the 1st International Conference on Emerging Trends in Energy Conservation – ETEC Tehran, Tehran, Iran, 2011.*
- [8] Luque. A and Hegedus. S.. "Handbook of Photovoltaic Science and Engineering". John Wiley & Sons Ltd, The Atrium, Southern Gate, Chichester, West Sussex PO19 8SQ, England, pp. 296-297, 2003.
- [9] David L. King, Jay A. Kratochvil, and William E. Boyson, "Temperature Coefficients for PV Modules and Arrays: Measurement Methods, Difficulties, and Results" the 26th IEEE Photovoltaic

- Specialists Conference, September, Anaheim, California, 1997.
- [10] David Tan Ang Kian Seng ‘Hand book of solar photovoltaic system (PV) systems’ , Singapore, 2011.
- [11] Radziemska, E.,” The effect of temperature on the power drop in crystalline silicon solar cells”, *Renewable Energy* 28, 1–12, 2003.
- [12] El-Shaer, A., M. T. Y. Tadros, M. A. Khalifa,” Effect of Light intensity and Temperature on Crystalline Silicon Solar Modules Parameters”, *International Journal of Emerging Technology and Advanced Engineering*, Volume 4, Issue 8, August 2014.

تأثير درجة الحرارة على انخفاض قدرة وحدات الخلايا الشمسية

قيس محمد عايش

معهد التكنولوجيا / بغداد

البريد الإلكتروني: Abdgold171@yahoo.com

الخلاصة

من اجل تحديد أي نوع من وحدات الخلايا الشمسية يكون استخدامها أفضل مع زيادة درجة الحرارة . تغير القدرة نتيجية زيادة درجات الحرارة (25°C, 35°C, and 45°C) تم ايجاده لثلاثة أنواع من وحدات الخلايا الشمسية وهي احادية التبلور، ثنائية التبلور، ونحاس- أنديوم- جليوم والسليناد الثنائي. لقد استعمل جهاز بروفا ٢٠٠ لتحليل الخلايا الشمسية لفحص وحدات الخلايا الشمسية الثلاث وفي درجات حرارة مختلفة : ٢٥ ، ٣٥ ، و ٤٥ درجة مئوية وضمن مدى اشعاع شمسي ١٠٠ الى ١٠٠٠ واط لكل متر مربع. وحدة الخلية نوع نحاس- أنديوم- جليوم والسليناد الثنائي هي الأقل انخفاض في قدرة 0.38%/°C بينما وحدة الخلية نوع احادية التبلور هي الاعلى 0.54%/°C . بينما وحدة الخلية متعددة التبلور كانت نسبة انخفاض الفولتية هي 0.49%/°C.